

Supporting Material

to

Visualization of the encounter Ensemble of the transient electron transfer complex of cytochrome *c* and cytochrome *c* peroxidase

Qamar Bashir, Alexander N. Volkov, G. Matthias Ullmann and Marcellus Ubbink

Coverage of the CcP surface using ten spin labels.

Centers of mass of Cc were positioned around CcP such that Cc just touched the CcP to provide a grid of points around CcP. In Figure S-1 a mesh is shown around CcP consisting of these points. For spin labels that do not affect any amide of Cc ($\Gamma_2 < 10 \text{ s}^{-1}$) it was estimated that the Cc cannot be within 8 Å of any of the four spin label orientations used to represent the spin label ensemble for more than 1% of the time. Given an average Cc radius of 14 Å, this implies that the center of mass of Cc must be $>22 \text{ Å}$ from the spin label. Thus, in the grid all points within 22 Å are shown in blue to show surface area that is occupied by Cc for less than 1% of the time. In red are shown the same areas with spin labels for which PREs were detected, representing the maximal area possibly sampled by Cc. It can be seen that the theoretical ensemble (magenta spheres) stays almost completely within this area. The yellow surface represents spin label attached to S263C for which a few small PREs were observed, suggesting that this spin label borders the area visited by Cc. Also shown is the same analysis for the set of spin labels used in an earlier study (ref. 13 in the main text). Note that the blue area take priority of red/yellow. With ten solvent accessible and flexible spin labels and the criteria given above, almost the entire surface area of CcP (13097 Å²) is covered, indicating that about 1300 Å² can be covered per spin label for this globular protein.

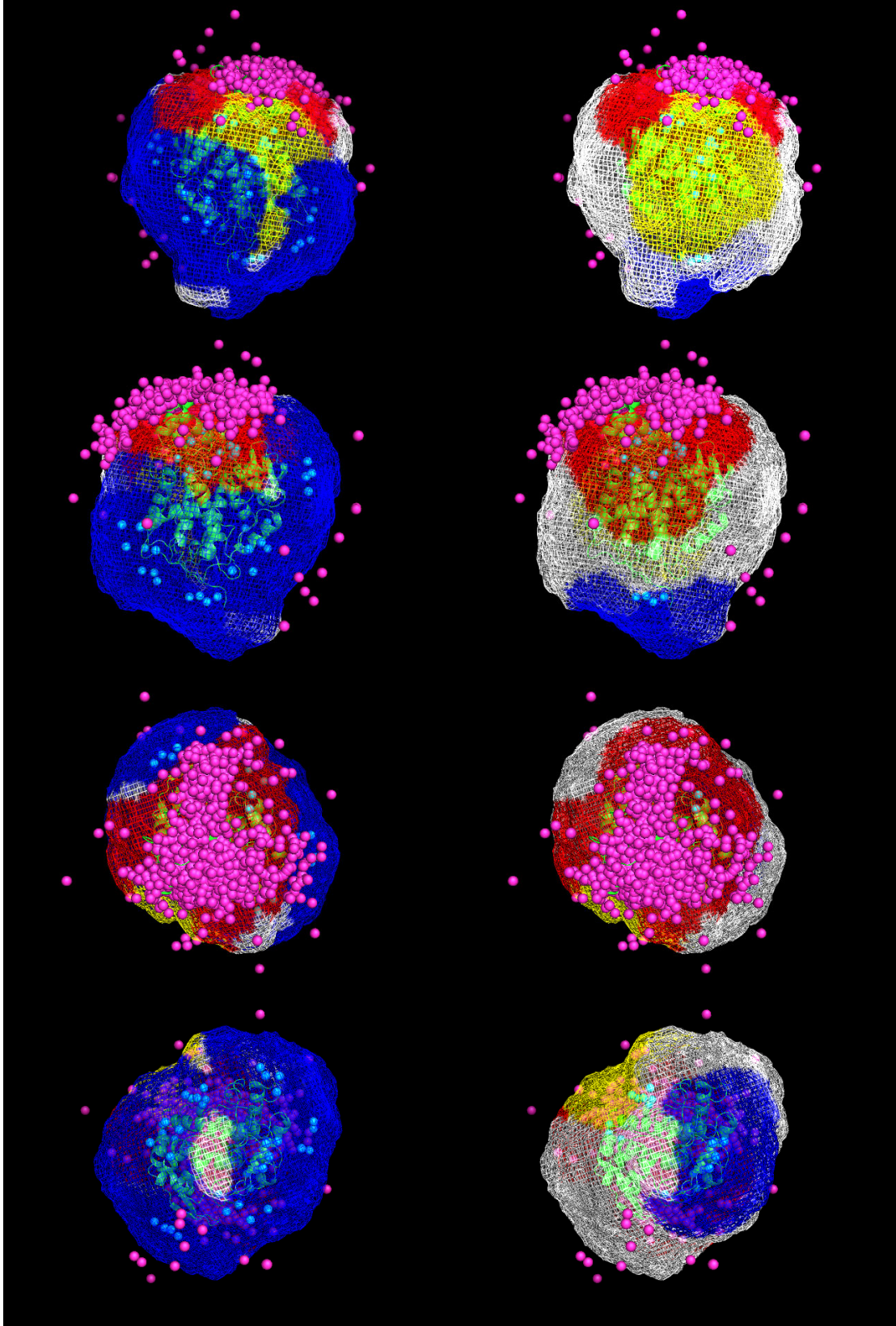


Figure S-1. Coverage of encounter complex sampling by Cc on CcP for the current study (left column) and earlier work (right column, ref. 13 in the main text). A grid of possible Cc positions around CcP is shown as a mesh, coloured according to the PRE data. The mesh around spin labels that cause no PRE on Cc is shown in blue, representing the surface of CcP in which Cc resides for less than 1% of the time. The red mesh represents the surface around spin labels that cause PRE, indicating the region that may be visited by Cc. In yellow is the mesh around the spin label attached to C263, which caused only a few small PRE effects. White mesh represent regions for which no data are available. The proteins in the specific complex are shown in green ribbons, the simulated encounter complex is shown as magenta spheres, representing the centers of mass of Cc. The oxygen atoms of the MTSL are shown as cyan spheres, with four atoms per spin label position, representing the four orientations used in the calculations. The images in each column represent different views. The view is the same for each left and right image.

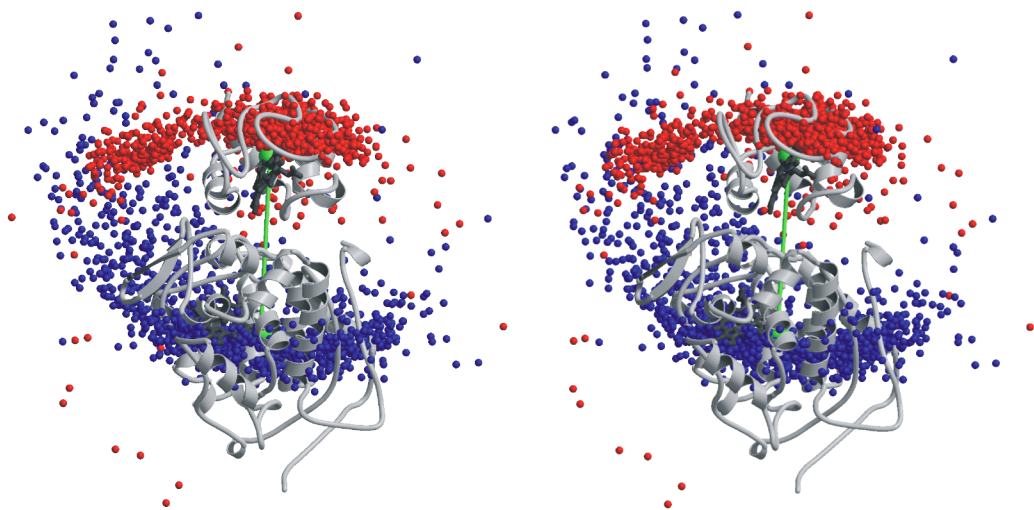
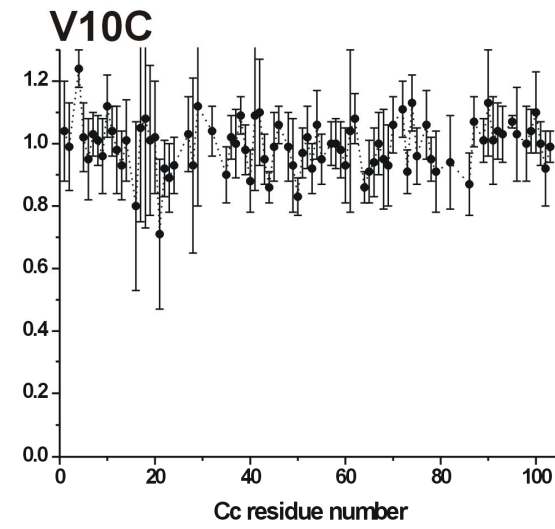
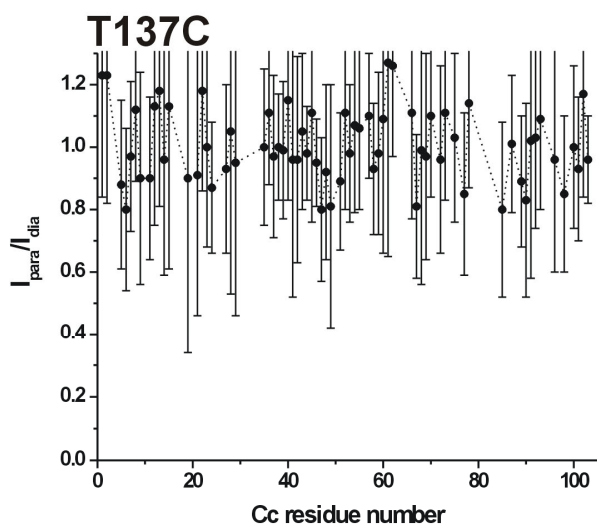
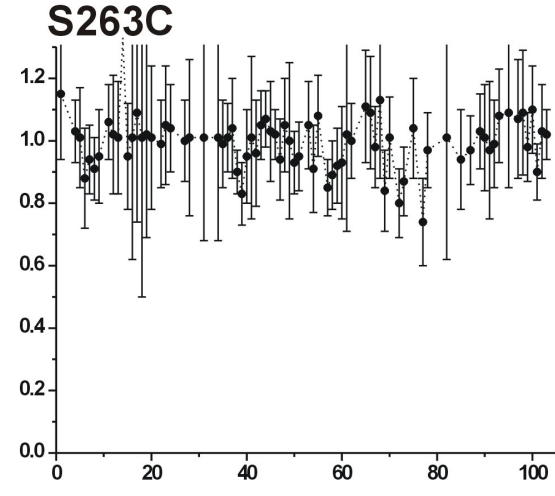
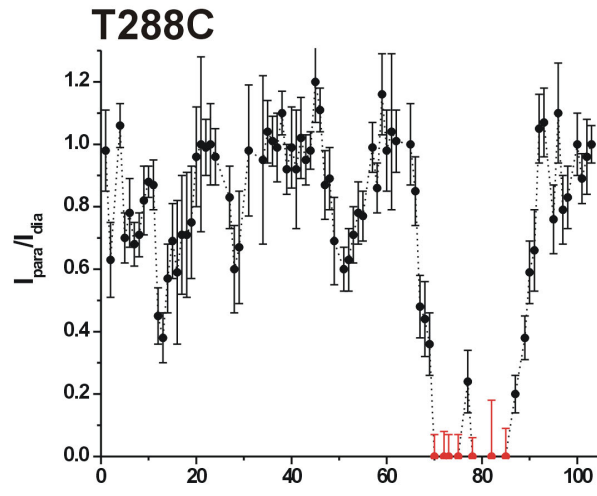
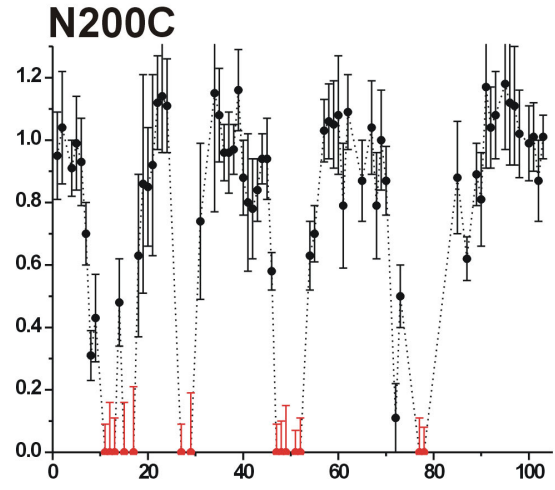
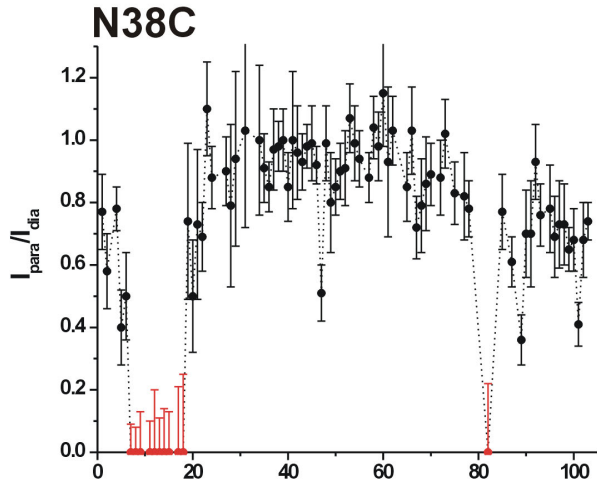


Figure S-2. Stereo representation showing distributions of Cc and CcP around the partner protein in the simulated encounter state superimposed on the specific complex. Red spheres show the centers of mass of Cc around CcP. Blue spheres show the centers of mass of CcP around Cc. Cc and CcP in the specific complex are shown as ribbons and heme shown as sticks. The centers of mass of the two proteins in the specific complex are shown as green spheres which are connected by the green line.



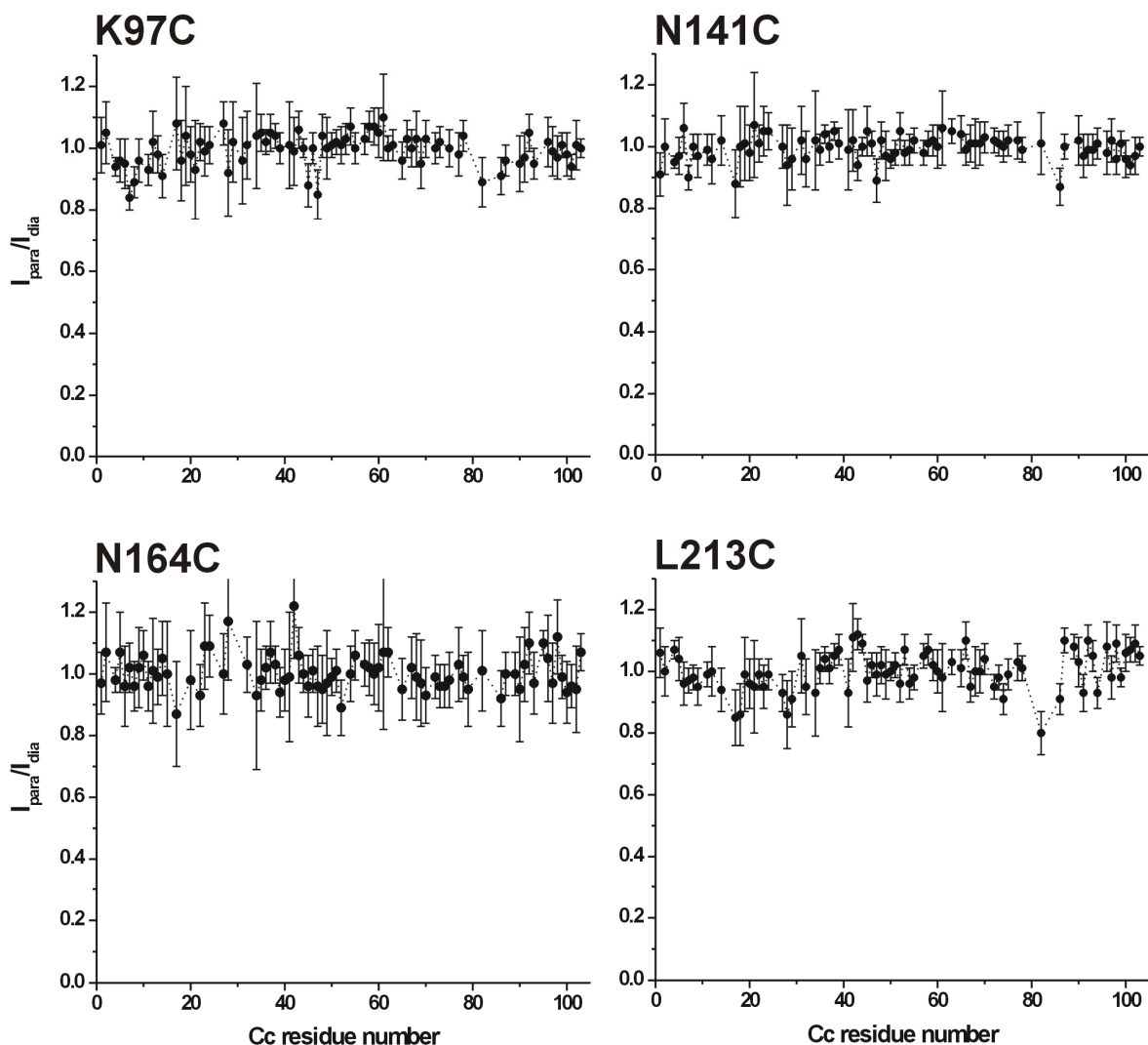


Figure S-3. PREs from CcP-SL on Cc. Relative [^1H , ^{15}N] HSQC intensities of Cc backbone amides in the complex with CcP labeled with a paramagnetic spin label (I_{para}) or a diamagnetic analogue (I_{dia}) at positions N38C, N200C, T288C, V10C, K97C, T137C, N141C, N164C, and L213C. For the residues whose resonances disappear in the paramagnetic spectrum (red), the upper limit of $I_{\text{para}}/I_{\text{dia}}$ was estimated from the noise level. The error bars denote standard deviations, derived from spectral noise levels using standard error propagation procedures.

Reference 37.

MacKerell, A. D.; Bashford, D.; Bellott; Dunbrack, R. L.; Evanseck, J. D.; Field, M. J.; Fischer, S.; Gao, J.; Guo, H.; Ha, S.; Joseph-McCarthy, D.; Kuchnir, L.; Kuczera, K.; Lau, F. T. K.; Mattos, C.; Michnick, S.; Ngo, T.; Nguyen, D. T.; Prodhom, B.; Reiher, W. E.; Roux, B.; Schlenkrich, M.; Smith, J. C.; Stote, R.; Straub, J.; Watanabe, M.; Wiorkiewicz-Kuczera, J.; Yin, D.; Karplus, M. *J. Phys. Chem. B* **1998**, *102*, 3586-3616.